J Mater Sci (2010) 45:6586–6592
DOI 10.1007/s10853-010-4747-2

Statistical analysis of the fracture strengths of aluminum alloy–alumina (Al_2O_3) particulate composites

A. Suresh babu · V. Jayabalan

Received: 6 January 2010 / Accepted: 1 July 2010 / Published online: 14 July 2010

Abstract The mechanics of composite materials and their "fracture behaviors" are relatively complex phenomena to analyze and establish due to their inconsistent process stability and reliability, combined with production and related processing problems. In this work, an attempt has been made to statistically analyze the tensile behavior of metal matrix composites. Composites of aluminum alloy containing 5–20% volume fraction of Al_2O_3 particles of 15 μm size were prepared by adding alumina particles to a vigorously agitated semi-solid aluminum alloy. Prior to this, alumina particles were subjected to preheating at 800 °C for 5 h. Particles were then added to the aluminum alloy and further heated to 850 °C by using a mixer in a nitrogen medium. A total of 20 tension tests were performed for each volume fraction according to ASTM Standards B557 and using these test data, the initial estimators for an empirical model were obtained. Using this empirical model, the reliability of the composite characteristics in terms of its tensile strength was assessed. Another significant implication of the present study is proving the ability and utility of the Weibull statistical distribution for describing the experimentally measured data on the tensile strength of metal matrix composites, in a more appropriate manner.

List of symbols

γ	Location parameter
α	Scale parameter
β	Shape parameter
$F(x; \alpha; \beta)$	Distribution function
$R(x; \alpha; \beta)$	Reliability function
n	Observation number
$x(i)$	ith order statistic

A. Suresh babu (✉) · V. Jayabalan
Department of Manufacturing Engineering, College of Engineering Campus, Anna University Chennai, Chennai 600025, India
e-mail: subaceg@gmail.com

Introduction

Al alloy matrix composites are more suitable option for application in Aerospace and Automobile Industries due to their light weight, higher specific modulus, specific strength, and resistance to wear characteristics [1–4]. In spite of these attractive characteristics, Al matrix composites were put to limited use in very specific application areas such as military weapons manufacturing and in Aerospace Industry products owing to its high manufacturing cost, complex fabrication process, and associated defects. However, of late Al matrix composites are being increasingly utilized for manufacturing automobile products and ancillaries such as engine pistons and cylinder liners, to make use of its improved mechanical properties and also on cost considerations [5]. Fabrication process methods of Al matrix composites can be classified as solid state process and liquid state process. A majority of products for commercial applications are now produced by liquid state process. The gravity mold casting, sand casting, and squeeze casting of liquid state processes are customarily used as fabrication methods of Al matrix composites. Stir casting process has been widely adapted to the fabrication of alumina particulate dispersed Al matrix composites [6–8]. Although many articles in the literature focus on the mechanical behavior of Al alloy matrix composites, only very few of them concerned with the "Reliability" characteristics of the composites. Generally, Al alloy composites demonstrate varied brittle fracture modes and

do exhibit scattered fracture strengths depending on the "volume fraction" of the particulate, the fabrication process, and its condition. Hence, the composites materials have not been widely used as the core structural material due to the above factors resulting in low reliability. Therefore, studies on the reliability and statistical strength analysis exercises have become essential and necessary for assuring and improving the quality in the composite material based products. It is also observed that most of these statistical strength analysis exercises make use of the Weibull distribution function equation [9–11]. The Weibull equation is based on the theory that fracture in a composite is controlled by the weakest defect among all the defects in a material, which is called the "Weakest Link theory." Hence, in this work, we performed the statistical analysis for the determination of the strength of the stir cast alumina/al alloy composites, using Weibull distribution function equations for predicting its reliability. Besides the above, micro-structural analysis was also performed to further evaluate the critical features of the composites.

Experimental procedure

Materials

The aluminum alloy used in this work is obtained in the form of ingots. The composition of the matrix material is shown in Table 1.

The properties of the reinforcement material (Al_2O_3) are:

- density : 3.97 gm/cc;
- elastic modulus : 393 GPa;
- hardness : 2100 KH (100 gm load).

Specimen preparation

The aluminum alloy metal matrix composite (MMC) was prepared using stir casting method using aluminum ingots in the proportion as detailed above. The ingots were melted in the primary furnace. Simultaneously, a second crucible with alumina particles containing 5–20% volume fraction of 15 μm size were pre-heated in a second furnace. After complete melting of the charge in the primary furnace, slag was removed if any. De-gasifiers for removing gas pockets and flux, to prevent oxidation was added to the charge.

Table 1 Chemical composition of Matrix Material

Material	Cu	Mg	Si	Fe	Mn	Ni	Zn	Pb	Sn	Al
%	0.03	0.03	0.3	0.4	0.03	0.03	0.07	0.03	0.03	Balance

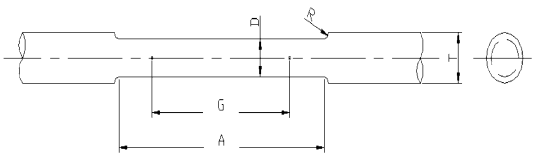

Fig. 1 Tensile specimen, where *G*—gauge length (45 mm), A—length of the reduced section (54 mm), *D*—nominal diameter (9 mm), *R*—radius of the fillet (8 mm), *T*—diameter of the rod (12 m)

After the release of reactive gases, the impeller was immediately introduced at 2/3 height [12] from the top of melt surface into the crucible and stirring was carried out. The pre-heated powder was introduced in the vortex formed in the molten metal. The die was properly placed in position to receive the molten composite from the tilting furnace. Immediately after stirring, the impeller was removed and the furnace was tilted to pour out the molten composite to the die to cast slab of size 150 × 100 × 25 mm. Set of specimens consisting of 20 test samples were prepared as per ASTM standards [13]. The entire set of specimens consisting of these samples were tested. A corner of each specimen was chosen for microstructure. Tensile tests were also carried out for representative specimen (Fig. 1) from aluminum alloy with 0% volume fraction of alumina reinforcement, for evaluating the "tensile strength" with the given casting conditions. Similarly the tensile tests for evaluating the tensile strengths, i.e., the fracture strengths, for other sets of 20 prepared specimens for volume fractions 5, 10, 15, and 20% were also conducted, and the results are tabulated (Table 2).

Weibull modeling

The term reliability in terms of probability of survival is used for the assessments of functional performance of a part under current service condition and in definite time period. The tensile strength of the composite materials was scattered widely because of their anisotropy. Hence safe life, i.e., reliability is an important parameter for this type of structure. Weibull distribution is being used to model extreme values such as failure times and fracture strength. Two popular forms of this distribution are two-parameter and three-parameter Weibull distributions. The (cumulative) distribution function of the three-parameter Weibull distribution is given as follows [14]:

$$F(x;\gamma,\alpha,\beta) = 1 - e^{-[(x-\gamma)/\alpha]\wedge\beta}, \quad \gamma \geq 0,\ \alpha \geq 0,\ \beta \geq 0 \quad (1)$$

where γ, α, and β are the location, scale, and shape parameters, respectively. When $\gamma = 0$ in Eq. 1, the distribution function of the two-parameter Weibull distribution is obtained. In this study, the two-parameter Weibull distribution, which can be

Table 2 Fracture strength values from tension tests

Sample no.	Tensile strength (Ts)				
	0%	5%	10%	15%	20%
1	91.6	130.5	140.1	115.5	100.6
2	91.6	132.3	142.3	115.5	101.6
3	92.0	134.4	142.3	123.8	102.3
4	92.3	134.4	142.3	123.8	102.5
5	92.5	134.5	142.3	124.7	102.6
6	92.6	136	142.5	124.7	102.6
7	92.8	136.8	142.5	130.4	103.5
8	93	136.8	142.8	130.4	103.6
9	93.6	137	143.2	131.8	103.6
10	93.7	137.6	143.5	131.9	104.2
11	94	138.2	143.5	134.4	104.5
12	94.5	138.2	145.2	134.8	104.9
13	94.6	139	145.2	143.5	104.6
14	95	139.5	145.2	143.5	105.6
15	95	139.5	145.3	143.6	105.6
16	95	142	145.6	143.6	106.3
17	95.6	145	146.3	145.7	106.5
18	95.6	146	146.3	146.8	107.6
19	97	148	146.5	149.2	108.4
20	98.7	150.6	147.2	158.3	109.5

used in fracture strength studies, will be considered. When $\gamma = 0$, the distribution function can be written as follows:

$$F(x;\alpha,\beta) = 1 - e^{-[(x/\alpha)\wedge\beta]}, \quad \alpha \geq 0,\ \beta \geq 0. \tag{2}$$

In the context of this study, $F(x;\ \alpha,\ \beta)$, represents the probability that the fracture strength is equal to or less than x. Using the equality $F(x;\ \alpha,\ \beta) + R(x;\ \alpha,\ \beta) = 1$, the reliability $R(x;\ \alpha,\ \beta)$, that is, the probability that the fracture strength is at least equal to x [15], is defined as:

$$R\,(x;\alpha,\ \beta)\ = e^{-(x/\alpha)\wedge\beta}, \quad \alpha \geq 0,\ \beta \geq 0. \tag{3}$$

The parameter α and β of the distribution function $F(x;\ \alpha,\ \beta)$ are estimated from the observations. The methods usually employed for the estimation of these parameters are the method of linear regression, method of maximum likelihood, and method of moments. Among these methods, linear regression, mostly adopted by practitioners, is used for parameter estimation in this article also. This method is based on transforming Eq. 2 into $1 - F(x;\ \alpha;\ \beta) = \exp\,[(x/\alpha)\wedge\beta]$ and taking the double logarithms of both sides. Hence, a linear regression model in the form $Y = mX + r$ is obtained:

$$\ln[\ln(1/(1 - F(x;\alpha,\beta))] = \beta\ln(x) - \beta\ln(\alpha). \tag{4}$$

$F(x;\ \alpha;\ \beta)$ is an unknown in Eq. 4 and, therefore, it is estimated from observed values: order n observations from smallest to largest, and let $x(i)$ denote the ith smallest observation ($i = 1$ corresponds to the smallest and $i = n$ corresponds to the largest). Then, a good estimator of $F(x(i);\ \alpha,\ \beta)$ is the median rank (M.R) of $x(i)$:

$$F(x(i);\alpha,\beta) = [(i - 0.3)/(n + 0.4)]. \tag{5}$$

When linear regression is applied to the paired values based on the least squares minimization, for the model in Eq. 4, the parameter estimates α and β are obtained:

$$(X, Y) = (\ln(x(i), \ln[\ln(1/(1 - F(x(i);\alpha,\beta))]).$$

In order to compute α and β, first, they are ordered from the smallest to the largest and $(X,\ Y)$ values are computed [16]. Then, applying linear regression to these $(X,\ Y)$ values, the linear regression model with the regression lines for various fractional volumes (Fig. 2) is obtained. Weibull parameters and the reliability values calculated for the present work are presented in Table 3.

Taking the 15% volume fraction as an example, the slope of the line is found to be 13.07 (as per Fig. 2a), which is the value of the shape parameter β. The equation $\beta < 1.0$ indicates that the material has a "decreasing" failure rate. Similarly $\beta = 0$ indicates constant failure rate and $\beta > 1.0$ indicates an "increasing" failure rate. The α value is computed as $\alpha = 140.07$ using the point, the line intersects the Y axis (=−64.63) in $\alpha = e^{(-Y/\beta)}$. Therefore, $\beta = 13.07$ indicates that the material tends to fracture

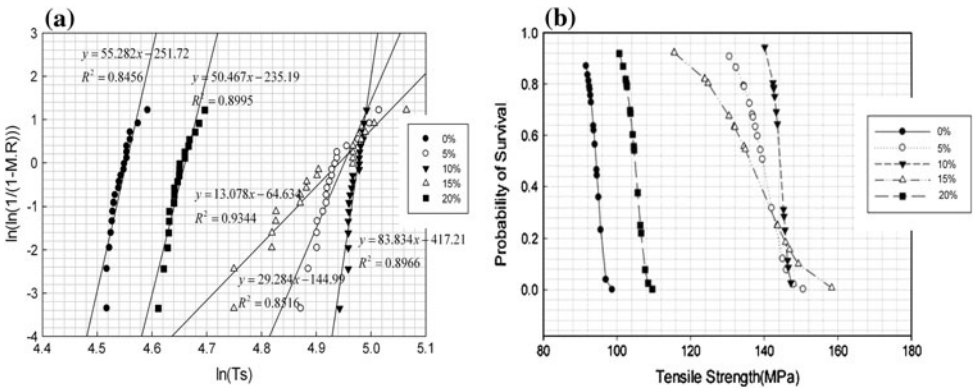

Fig. 2 **a** Regression model and **b** probability of survival

Table 3 Weibull parameters and reliability values

Volume fraction (%)	Tensile strength (Ts)	$X = \ln$ (Ts)	Median rank (M.R)	$Y = \ln(\ln (1/(1 - \text{M.R})))$	$R(t)$
0	91.62	4.51765	0.034314	−3.3548025	0.87
	91.62	4.51765	0.083333	−2.4417164	0.87
	92.052	4.522354	0.132353	−1.9521377	0.835
	92.3	4.525044	0.181373	−1.6088072	0.812
	92.5	4.527209	0.230392	−1.3398911	0.79
5	130.546	4.871726	0.034314	−3.3548025	0.907
	132.37	4.885601	0.083333	−2.4417164	0.864
	134.46	4.901267	0.132353	−1.9521377	0.793
	134.476	4.901386	0.181373	−1.6088072	0.793
	134.56	4.90201	0.230392	−1.3398911	0.789
10	140.125	4.942535	0.034314	−3.3548025	0.944
	142.36	4.958359	0.083333	−2.4417164	0.805
	142.365	4.958394	0.132353	−1.9521377	0.804
	142.365	4.958394	0.181373	−1.6088072	0.804
	142.365	4.958394	0.230392	−1.3398911	0.804
15	115.533	4.749556	0.034314	−3.3548025	0.923
	115.55	4.749703	0.083333	−2.4417164	0.922
	123.8	4.818667	0.132353	−1.9521377	0.82
	123.844	4.819023	0.181373	−1.6088072	0.819
	124.711	4.825999	0.230392	−1.3398911	0.803
20	100.63	4.61145	0.034314	−3.3548025	0.919
	101.65	4.621536	0.083333	−2.4417164	0.869
	102.365	4.628545	0.132353	−1.9521377	0.818
	102.563	4.630477	0.181373	−1.6088072	0.802
	102.66	4.631423	0.230392	−1.3398911	0.793

with higher probability for every unit increase in applied tension. The scale parameter α measures the spread in the distribution of data. As a theoretical property, $R(\alpha; \alpha, \beta) = 0.367$ (as per Eq. 3). Therefore, R (140.07; 140.07, 13.07) $= e^{[(x/\alpha)\wedge\beta]} = 0.378$, that is 36.8% of the tested specimens have a fracture strength of at least 140.07 MPa. The plot of $R(x; \alpha; \beta)$ is shown in Fig. 2. The probability of survival plot Fig. 2 shows that fracture strength values roughly less than or equal to 115 MPa will prove high for their reliability at a volume fraction reinforcement of 15%. For more precise assessment, the reliability values 0.90 and 0.95 were considered and when these values are put as $R(x; \alpha, \beta)$ in Eq. 3 and the equation is solved for x, the fracture strength values 117.9 and 111.5 are obtained, respectively. In other words, this material will fracture with 0.90 probability for a fracture strength value of 117.9 MPa or more, and similarly will fracture with 0.95 probability for a tension of 111.5 MPa or more. Similarly the values 92, 131, 140, and 105 MPa were proved high to be reliable for 0, 5, 10, and 15%, respectively. Also we can observe that reinforced MMCs at 10% volume fraction level offers more strength with high reliability.

Coefficient of variation (CV), standard deviation (SD), and mean strength to failure (MSTF) values for the fracture strength of MMC samples have been calculated by using Eqs. 6–8:

$$\text{Mean strength to failure} = \alpha\,\Gamma(1 + 1/\beta), \tag{6}$$

$$\text{SD} = \left(\alpha \cdot \sqrt{\Gamma(1 + 2/\beta) - \Gamma^2(1 + 1/\beta)}\right), \tag{7}$$

$$\text{CV} = \left(\alpha . \sqrt{\Gamma(1 + 2/\beta) - \Gamma^2(1 + 1/\beta)}\right)/(\alpha\,\Gamma(1 + 1/\beta)), \tag{8}$$

where Γ is the gamma function.

CV graph for mean life of different volume fraction reinforcement specimens has been shown in Fig. 3. According to the results so plotted, the scattered fracture strength is highest at 15% volume fraction. Another findings from Fig. 3 is that the 10% volume fraction level offers consistency (with minimum CV and high reliability and strength).

Empirical model

An empirical model (Eq. 9) was developed based on Weibull distribution and the parameter estimates ($R^2 =$

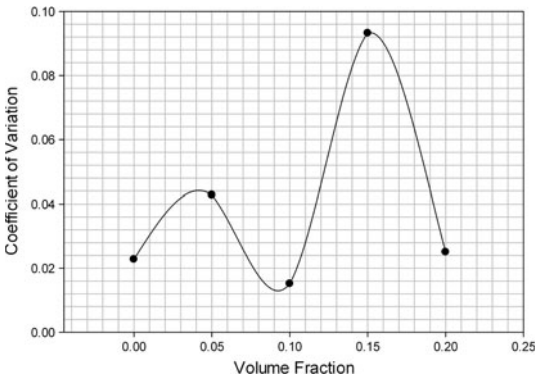

Fig. 3 Coefficient of variation

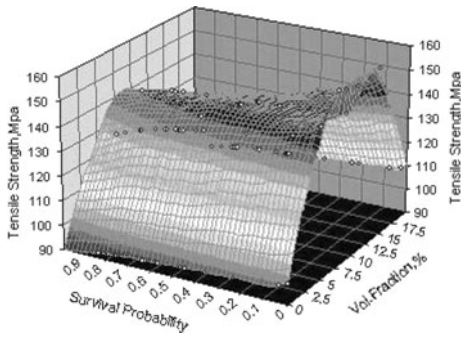

Fig. 4 The 3D graph for Al alloy–Al_2O_3 particulate MMC with various volume fractions

0.99) of the model for various vol.% reinforcement are tabulated in Table 4:

$$y = a + b\left[1 - \exp\left(-\left(\frac{x + \alpha(\ln 2)^{\frac{1}{\gamma}} - \beta}{\alpha}\right)^{\gamma}\right)\right]. \quad (9)$$

A 3D graph was drawn to predict the required values of tensile strength, volume fraction from the given two parameters as shown in Fig. 4.

Table 5 shows the error percentage for parameter evaluation culled from the given values between the empirical model and the 3D graph. The low residual percentages so arrived as per the table do indicate that 3D graphs can be a reliable tool to evaluate the parameter from the given values.

Microstructure study

The scanning electron microscope was used to examine and characterize the fine scale topography and microscopic mechanisms governing the fracture, where the observations pertain to the zones when the cracks originated. The study reveals that the distribution of the particles in the matrix is not as uniform as expected.

From the study, it can be inferred that the crack initiation starts at the zone of clustering of the particulates in the material. The failure caused by the effect of particle separation and initiation cum growth of particles–matrix interface "voids" could be due to the mechanical deformation of ductile aluminum metal matrix and the hard, brittle alumina reinforcing particles. Clustering of particulates in the composite material normally occur at a higher volume fraction. Hence, we can observe that the "stress amplitude," which is necessary to initiate "micro plastic deformation" in MMCs, is on the increase up to 10% volume fraction and then starts reducing beyond 10% volume fraction. This has resulted in the reduction in properties and reliability at a volume fractions of 15% and higher. The evolution of damage across the specimen gauge length throughout the loading history is very heterogeneous, while the final fracture does not typically occur where the damage level is highest on the surface of the specimen as mentioned in other literatures [17–20]. This indicates that the spatial distribution of damage in three dimensions are likely to be important for both nucleation and damage in such materials. Consistent with this, early work [18–23] illustrated that fracture nucleation in particulate composites typically occur in regions of clustered reinforcement, while crack propagation may be linked to defects contained in the clustered regions.

The tensile deformation of the composite shown in Fig. 5 indicate an overall rough surface and also an evidence of brittle failure. This might be attributed to the failure of the reinforcing particles and the dislodgement occurring at the ceramic particles–matrix interfaces. In the tested material, two different types of "dimples" were observed (Fig. 5b), those finer dimples immediately close to the reinforced particles and those associated with the second phase of coarse particles and intermetallics, which

Table 4 Parameter estimates

Parameters	Values				
	0%	5%	10%	15%	20%
a	0.986642494	0.999066054	0.998176756	0.999667641	1.000559453
b	−0.98758521	−0.99898933	−0.99964172	−0.99976538	−1.00047303
β	94.9531322	141.3451282	144.9754733	140.0660254	105.6765408
γ	37.25509462	131.0990958	90.41597210	138.1338130	112.0532900
α	55.28156061	29.2839537	83.83416472	13.07826796	50.46680718

Table 5 Evaluation of tensile strength by empirical model and surface graph

Index	Volume fraction	Survival probability	Tensile strength (MPa)		Error	%Error
			Surface model	Empirical model		
1	5	0.05	146.162	146.746	−0.5841	−0.39963
2	5	0.1	145.587	145.43	0.1567	0.107634
3	5	0.15	144.23	144.469	−0.2389	−0.16564
4	10	0.05	146.925	146.886	0.0392	0.02668
5	10	0.1	146.425	146.428	−0.0024	−0.00164
6	10	0.15	146.08	146.089	−0.0095	−0.0065
7	10	0.2	145.798	145.803	−0.0047	−0.00322
8	10	0.25	145.545	145.543	0.0022	0.001512
9	15	0.05	153.362	152.313	1.0491	0.68407
10	15	0.1	149.271	149.28	−0.0087	−0.00583
11	15	0.15	147.072	147.086	−0.0134	−0.00911
12	15	0.2	145.24	145.248	−0.0078	−0.00537
13	15	0.25	143.602	143.6	0.0013	0.000905
14	20	0.05	107.801	107.998	−0.1965	−0.18228
15	20	0.1	107.565	107.436	0.1283	0.119277
16	20	0.15	107.167	107.025	0.1415	0.132037
17	20	0.2	106.698	106.677	0.0211	0.019775
18	20	0.25	106.362	106.362	−0.0005	−0.00047

are much smaller and shallower. Coarse dimple formation is due to the deformation of matrix aluminum, while the fine dimples are due to ductile fracture in the remaining aluminum ligament. Large parts of the observed fracture surfaces showed microscopic fracture (Fig. 5d) of the base matrix material accompanied with the debonding of the

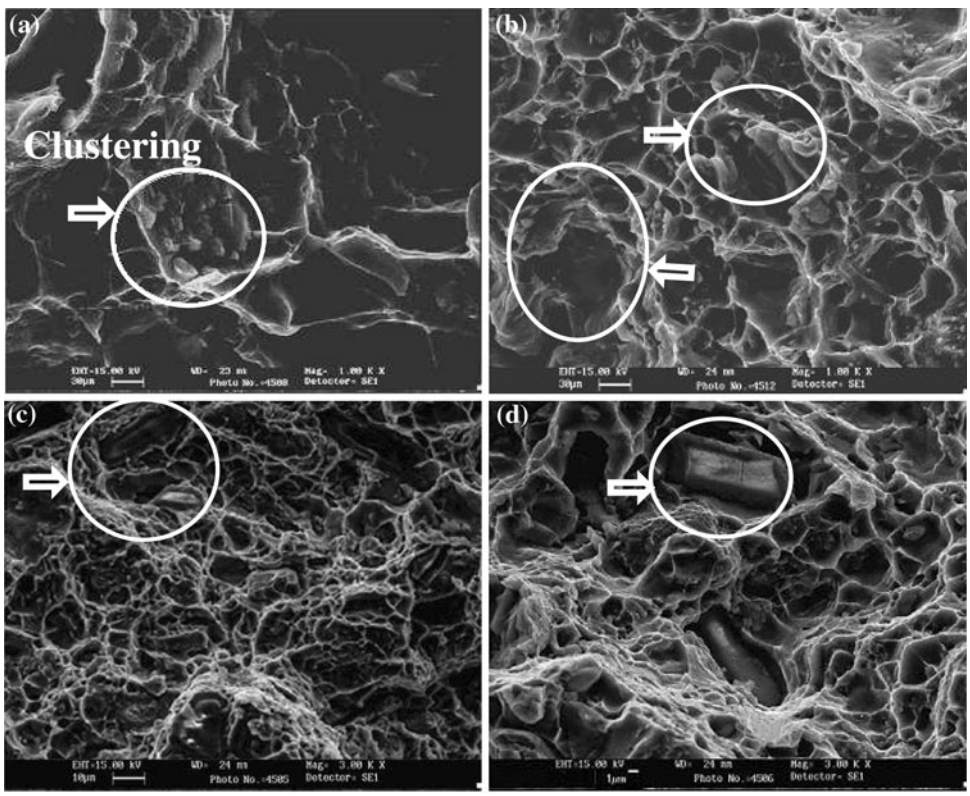

Fig. 5 SEM pictures: **a** fracture surface with clustering of the alumina particles (30 μm), **b** dimple formation on the fractured surface (30 μm), **c** debonding of the alumina particles (10 μm), **d** high resolution magnified view of debonded alumina particle (1 μm)

reinforcing alumina particles from the matrix. The failure is due to the particle–matrix interface voids that form during the mechanical testing, followed by link-up in the ductile aluminum matrix. As a consequence, a higher stress amplitude is required to initiate micro plastic deformation in the composites as compared to the unreinforced alloy due to the constraint provided by the particles, as shown elsewhere [21–23]. It appears that the main fracture mechanism is due to the large concentration of stress, which is close to the reinforcing particles, leading to cracks in the adjacent matrix and to a failure in a microscopically ductile manner.

Conclusion

In the present work, we have considered Weibull statistical distribution function with an aim to critically analyze the strength data of composite materials. The experimentally measured strength data obtained using aluminum–alumina (Al_2O_3) particulate composites were used to validate the statistical analysis. The implication of our study is in that the "strength of composite materials" could be effectively characterized using the empirical model based on Weibull statistical distribution function as detailed in Eq. 9. Here, the "two-parameter Weibull distribution" was used to find the initial estimates for designing the empirical model. The empirical model was then used to predict the strength values. To validate the empirical model further, we have used the "minimum error percentage" between predicted values and experimental values. Also a three-dimensional graph was used as an additional tool, along with the empirical model to predict the required values on tensile strength, volume fraction from the given two parameters. The low error percentages revealed by the empirical model indicate that the three dimensional graph could be a reliable tool to evaluate the required parameters from the given values with minimum deviation. In addition, the extreme maximum value distribution is in good agreement with the general physical understanding of the tensile behavior of aluminum–alumina (Al_2O_3) particulate composites. One of the significant advantages of the Weibull analysis method is that it allows a means of predicting the likelihood of failure of a material at low stress values, possibly allowing designers to select a material depending on the expected level of stress according to the requirement.

It is thus necessary to continue work of this nature for evaluating and developing new strength test methods that are more reliable for testing composite materials.

References

1. Young RMK, Clyne TW (1986) J Mater Sci 21(3):1057. doi:10.1007/BF01117395
2. Arsenault RJ, Taya M (1987) Acta Metall 35(3):651
3. Arsenault RJ, Wu SB (1988) Scr Metall 22(6):767
4. Everett RK, Arsenault RJ (1991) Metal matrix composites: mechanism and properties. Academic Press, San Diego
5. Schumacher CA (1989) SAE technical papers no. 892495
6. Jarry P, Michaud VJ, Mortension A, Dubus A, Tirard-collet R (1992) Metall Trans 23(8):2281
7. Lee TW, Kim SM, Suh JH, Lee CH (1997) In: Lee EW et al. (ed) Proceedings of the forth light weight alloys for aerospace applications symposium. The Minerals, Metals & Materials Society, Orlando, February 1997, p 265
8. Mochizuki S, Shiria H, Ohshiro J, Hino H, Ebe Y (1992) In: Proceeding of the 1992 Japan Die Casting Congress transactions, Japan Die Casting Association, p 228
9. Layden GK (1973) J Mater Sci 8(11):1581. doi:10.1007/BF00754893
10. Chi Z, Chou TW, Shen G (1984) J Mater Sci 19(10):3319. doi:10.1007/BF00271016
11. Martineau P, Lahaye M, Pailler P, Naslain R, Couzi M, Creuge F (1984) J Mater Sci 19:2731. doi:10.1007/BF00550832
12. Balasivanandaprabu S, Karunamoorthy L, Kathiresan S, Mohan B (2006) J Mater Process Technol 171:268
13. ASTM Standards (1989) Metal matrix composites—testing, analysis and failure. ASTM, Philadelphia
14. Hallinan A, Jr J (1993) J Qual Technol 25(2):85
15. Dodson B (1994) Weibull analysis. American Society for Quality, Milwaukee
16. Taljera R (1981) ASTM STP 723, p 291
17. Lloyd DJ (1991) Acta Metall Mater 39(1):59
18. Lewandowski JJ, Liu C (1988) Proceedings of international symposium on advanced structural materials, vol 2. Pergamon Press, Montreal, p 23
19. Lewandowski JJ, Liu C, Hunt WH Jr (1989) Mater Sci Eng A107:241
20. Singh PM, Lewandowski JJ (1993) Met Trans A 24A:2451
21. Lewandowski JJ, Liu DS, Manoharan M (1989) Met Trans A 20A:2409
22. Liu DS, Lewandowski JJ (1993) Met Trans A 24A:609
23. Lewandowski JJ, Liu DS, Liu C (1991) Scr Met 25(1):21